Compact and Low-Profile Linear-/Circular-Polarization Dielectric Resonator Antennas With Extended Bandwidths

JIE-ER ZHANG[1], **QINFANG ZHANG**[1], **WEIBIN KONG**[2], **WEN-WEN YANG**[3] **(Member, IEEE),**
AND JIAN-XIN CHEN[3] **(Senior Member, IEEE)**

[1]School of Materials Science and Engineering, Yancheng Institute of Technology, Yancheng 224051, China

[2]College of Information Engineering, Yancheng Institute of Technology, Yancheng 224051, China

[3]School of Information Science and Technology, Nantong University, Nantong 226019, China

CORRESPONDING AUTHORS: Q. ZHANG AND W.-W. YANG (e-mail: qfangzhang@gmail.com; wwyang2008@hotmail.com)

ABSTRACT The dielectric resonator antenna (DRA) with wide bandwidth, compact size and low profile is considered as an attractive candidate for 5G wireless communications. However, most of the reported DRAs either have bulky volumes or have limited bandwidths. In this paper, a kind of compact and low-profile DRA with extended bandwidth is proposed. By observing the E-field distribution differences between the two target modes and modifying the dielectric characteristics (such as material and dimension) of the designated region where the E-field is very weak for fundamental TE_{111} mode but quite strong for high-order TE_{131} mode, the frequency of TE_{131} mode can be significantly affected and shifted down to merge with that of TE_{111} mode which is less affected. As a result, extended operating bandwidth can be obtained. This technique also benefits from not having to enlarge the planar size of the high permittivity DR, therefore making the antenna compact enough for 5G beam-scanning and low profile applications. For demonstration, linear- and circular- polarization antenna prototypes were designed and measured. The LP antenna has a -10 dB impedance bandwidth of 17.3% and a peak gain of 7.1 dBi while the CP antenna achieves a 3-dB axial ratio (AR) bandwidth of 12% and a peak gain of 6.6 dBic. Both the antennas have compact volumes of no larger than $0.35\lambda_0 \times 0.35\lambda_0 \times 0.11\lambda_0$. Based on the LP and CP antenna elements, two 1×5 antenna arrays with the capability of beam scanning are designed and simulated. Wide scanning angles of $\pm45°$ and $\pm40°$ can be obtained for the LP and CP arrays, respectively.

INDEX TERMS Beam-scanning, circular polarization, compact, dielectric resonator antenna, linear polarization, low-profile, bandwidth.

I. INTRODUCTION

MASSIVE multiple-input multiple-output (MIMO) beam-scanning technology is considered as one of the key technologies in 5G to improve the spectrum efficiency [1]–[2]. Basically, this technology imposes some requirements on the antenna designs such as: 1) **High efficiency.** The large number of antennas and radio frequency (RF) channels lead to a sharp increase in

energy consumption. To improve the power efficiency, the antenna should have high efficiency. 2) **Wide bandwidth.** The antenna should have a wide bandwidth ($>15\%$, e.g., covering 5G n78 band) to support the high data throughput. 3) **Compact size.** To achieve good beam-scanning performance and avoid unwanted grating lobes, the antenna array spacing should be kept as about $0.5\lambda_0$ (λ_0 refers to the free space wavelength at center frequency). The planar

size of the array element is thus required to be compact ($<0.4\lambda_0 \times 0.4\lambda_0$) enough to fit the spacing demand [3]–[5]. Considering, also, the market demand for skinny and lightness devices, **low antenna profile** of less than $0.1\lambda_0$ is highly preferred.

Dielectric resonator antennas (DRAs) can achieve high radiation efficiency due to the absence of metallic losses. Additionally, they are lightweight, cost effective, and easy for excitation [6]–[8]. They are thus considered as suitable candidates for 5G communication systems. By using different strategies, many conventional DRAs can achieve wide operating bandwidths. However, most of the designs have bulky volumes [9]–[18], either large planar sizes ($>0.5\lambda_0 \times 0.5\lambda_0$) [9]–[13] or high profiles ($>0.3\lambda_0$) [14]–[18]. To reduce the antenna profile, some novel low profile DRA configurations such as dense dielectric patch resonator antenna (DDPA) [19]–[20] and planar DRA [21] have been proposed recently. Nevertheless, owing to the use of high permittivity dielectric materials, such DRAs usually have high radiation Q-factors, leading to limited operating bandwidths (typically less than 5%) [22]. Several methods have been proposed to broaden the bandwidths of the antennas. In [23]–[24], the length-to-height ratios of the antennas are increased to make the high-order modes be merged with the low-order modes. In [25]–[26], the DRA mode and the feeding slot mode are skillfully combined to enhance the bandwidth. In [27]–[29], stacked structures are employed to achieve broadened bandwidths. In [30], parasitic elements are introduced to acquire a wideband response. In [31], a differential parallel feeding structure is proposed to increase the operating bandwidth. These methods can effectively improve the operating bandwidths, but still at the cost of enlarging either the planar sizes or the profiles of the antennas, thereby limiting their applications.

With the above background, we proposed a kind of compact ($0.35\lambda_0 \times 0.35\lambda_0$) and low profile ($\sim 0.1\lambda_0$) DRA solution with **wideband** figure of merit since most of the similar-sized DRAs have very narrow bandwidths while majority of the wideband designs suffer from bulky volumes. The antenna uses high permittivity dielectric materials, thus featuring low antenna profile. By modifying the dielectric characteristics (such as material and dimension) of the designated region of a square high permittivity dielectric sheet, the resonant frequency of high-order TE_{131} mode can be effectively shifted down to be close to the fundamental TE_{111} mode. Combining the two modes can greatly enhance the operating bandwidth. Notably, the merge of the two modes is done on the premise of a fixed antenna planar size, which can be compact enough for beam-scanning applications.

Circularly polarized (CP) antennas are often used to reduce multipath interferences and ensure the communication reliability [32]–[34]. Some techniques have been proposed to realize the CP radiation with compact DRA structures [35]–[37]. However, the axial ratio (AR) bandwidths are still limited. In this paper, a compact and low-profile

TABLE 1. Performance comparison between the previous antennas and LP-/CP antennas in this article.

Ref	Published Year	BW (%)	AR (%)	DR Size ($\lambda_3 0$)	Gain (dBi/dBic)
[23]	2015	40	-	0.77×0.77×0.1	10.5
[24]	2020	4.9	-	0.51×0.51×0.05	8.75
[25]	2014	10.5	-	0.5×0.5×0.04	6.75
[26]	2016	14.5	-	0.37×0.37×0.18	5.1
[27]	2020	15	-	0.4×0.4×0.2	8
[29]	2018	9.7	-	1.17×1.17×0.15	9.7
[30]	2019	12	-	1.6×0.5×0.04	7.6
[31]	2018	12.5	-	0.2×0.22×0.2	6.6
This work (LP)		**17.3**	**-**	**0.35×0.35×0.07**	**7.1**
[26]	2016	15.4	6.1	0.37×0.37×0.18	4.7
[35]	2018	51	8	0.72×0.72×0.25	5
[36]	2021	7.3	5.5	0.34×0.34×0.17	7.1
[37]	2021	13.8	9.7	0.44×0.44×0.07	7.6
This work (CP)		**17.5**	**12**	**0.35×0.35×0.11**	**6.6**

λ_0 means the free-space wavelength at the center frequency f_0.

CP DRA with extended AR bandwidth is also investigated based on the same principle with the LP counterpart.

For demonstration, both the LP and CP DRAs were designed at 10 GHz for universality. In each case, a prototype was fabricated and measured. Reasonable agreement between the measured and simulated results was obtained. Table 1 lists the comparisons between the proposed antennas and previous works. For LP design, compared to [24]–[27] and [29]–[30], the proposed antenna has a more compact size and a wider bandwidth. Although the antenna in [23] has wider bandwidth and higher gain, its planar size is quite large, making it unsuitable for beam-scanning applications. The antenna in [31] has a smaller planar size, but its profile is too high. For CP design, it is learned that the proposed antenna has a more compact volume and a wider AR bandwidth than that in [26] and [35]–[37].

II. LINEARLY POLARIZED ANTENNA DESIGN
A. ANTENNA CONFIGURATION
The geometric configuration of the proposed LP antenna is exhibited in Fig. 1, which can be divided into two sections: radiation part on the top and feed structure in the bottom. The radiation part consists of one dielectric sheet, two dielectric strips and a substrate layer of Sub1. The feed structure is integrated in another substrate layer of Sub2. To excite the antenna, an H-shape slot is etched at the ground plane on top of Sub2, below which a microstrip line is deployed with a quarter-wave transformer introduced for tuning impedance matching. Both the dielectric sheet and dielectric strips are made of high permittivity ceramic materials with material of $\varepsilon_{r1} = 45$ and $\tan\delta = 1.9 \times 10^{-4}$ for the former and that of $\varepsilon_{r2} = 69$ and $\tan\delta = 2.7 \times 10^{-4}$ for the latter. Sub1 and Sub2 are made of Rogers 4003C laminates ($\varepsilon_{r3} = 3.55$ and $\tan\delta = 0.0027$). The dielectric materials are cemented onto the upper surface of Sub1 by using glue while the two
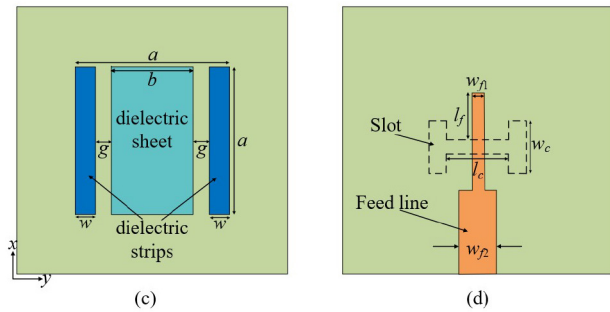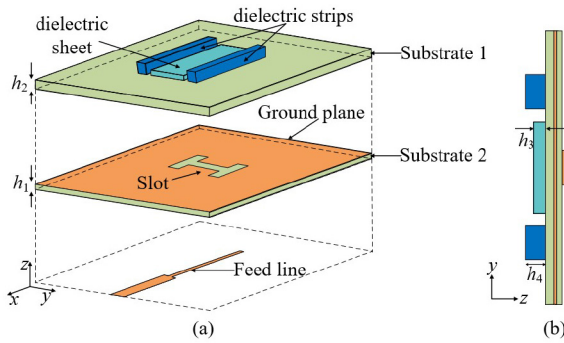
FIGURE 1. Configuration of the proposed LP DRA. (a) 3-D view. (b) Side view. (c) Top view. (d) Bottom view. (Design parameters: $h_1 = 0.508$, $h_2 = 0.813$, $h_3 = 0.56$, $h_4 = 1.2$, $a = 10$, $b = 5.6$, $w = 1.4$, $g = 0.8$, $w_c = 2$, $w_{f1} = 0.65$, $w_{f2} = 1.2$, $l_c = 2.5$, and $l_f = 2.05$. Units: mm.)
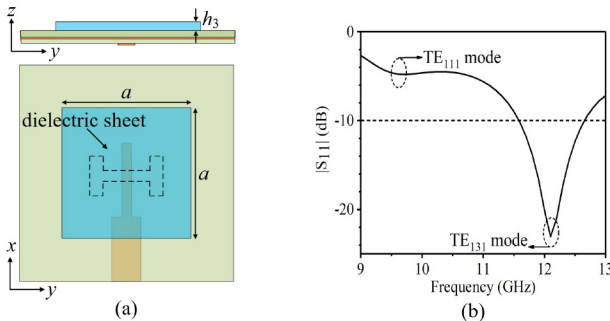

FIGURE 2. Configuration and simulated results of the conventional low profile DRA. (a) Antenna Configuration. (b) Simulated $|S_{11}|$.

FIGURE 3. Simulated E-field distributions of the two modes on XOY-plane of the dielectric sheet. (a) TE_{111} mode. (b) TE_{131} mode.

FIGURE 4. Simulated results of the LP DRA. (a) Frequencies of the two modes against ε_{r2} under different g. (b) f_{TE111}/f_{TE131} against ε_{r2} under different g.

substrate layers are bonded together using a prepreg layer of Rogers 4450B ($\varepsilon_{r3} = 3.54$, $\tan\delta = 0.004$).

B. ANALYSIS OF A CONVENTIONAL LOW PROFILE DRA

To explain the reason of modifying dielectric characteristics in the particular region of a square dielectric sheet, the mode behavior of a conventional low profile DRA with an intact high permittivity dielectric sheet should be analyzed firstly. Fig. 2 shows the analysis model and its simulated reflection coefficients. The DRA model has a square dielectric sheet with $\varepsilon_{r1} = 45$ and $\tan\delta = 1.9 \times 10^{-4}$, whose volume is $a \times a \times h_3$. To fit the beam-scanning usage, the side length a is set as $0.35\lambda_0$, where λ_0 corresponds to the free-space wavelength at 10 GHz. With h_3 determined as 0.56mm, the DRA can provide two resonances at 9.6 GHz and 12.2 GHz, respectively. Fig. 3 presents the E-field distributions at the two resonant frequencies, indicating that the first resonance
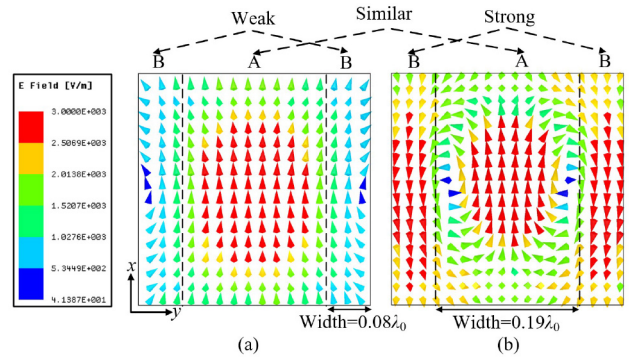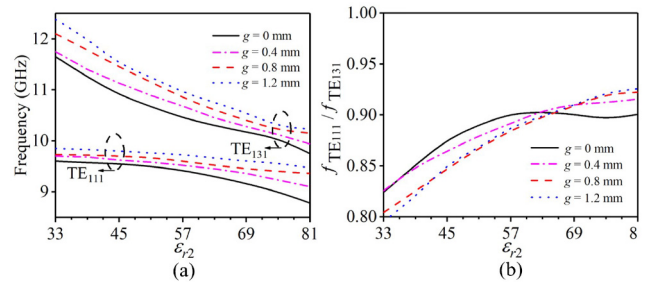
is caused by the fundamental TE_{111} mode while the second one is due to the high-order TE_{131} mode. The two modes, at this stage, are far apart from each other in the frequency axis due to the very compact DR planar size [10].

Comparing the E-field distributions, it can be observed that the two modes have very similar field intensity distribution in Region A but quite different intensity distribution in Region B. Specifically, the width of region B is around $0.08\lambda_0$, and in this region the strength of the E-field distribution of TE_{131} mode is much stronger than that of the TE_{111} mode. Therefore, we can predict that modifying the dielectric characteristics of Region B will have less influence on TE_{111} mode but have significant influence on TE_{131} mode. Based on this principle, we propose the design strategy in the following part for bandwidth extension.

C. DESIGN STRATEGY

Fig. 1 shows that in Region B, the dielectric material and its dimension have been modified, forming two dielectric strips along with the air gaps. Specifically, we introduce three controllable variables for analysis: permittivity of the dielectric strips ε_{r2}, size of the air gap g, and height of the dielectric strip h_4. Note that g and strip width w are inter-connected, that is when g increase, w will decrease accordingly since the sum of them is kept as the width of region B ($g + w = 0.08\lambda_0$). The planar size of the modified DR is still $a \times a$, where a is $0.35\lambda_0$.

Fig. 4(a) shows the simulated frequencies of TE_{111} mode and TE_{131} mode against ε_{r2} and g by the eigen mode
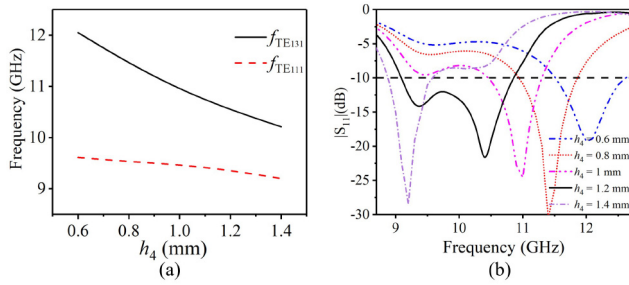
FIGURE 5. Simulated results of the LP DRA. (a) Frequencies of the two modes with different h_4. (b) Merging process of the two modes.
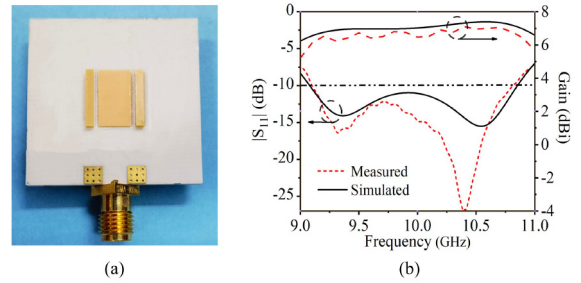

FIGURE 6. Photograph and measured results of the LP DRA. (a) Photograph of the fabricated antenna (b) Simulated and measured $|S_{11}|$ and gains of the antenna.
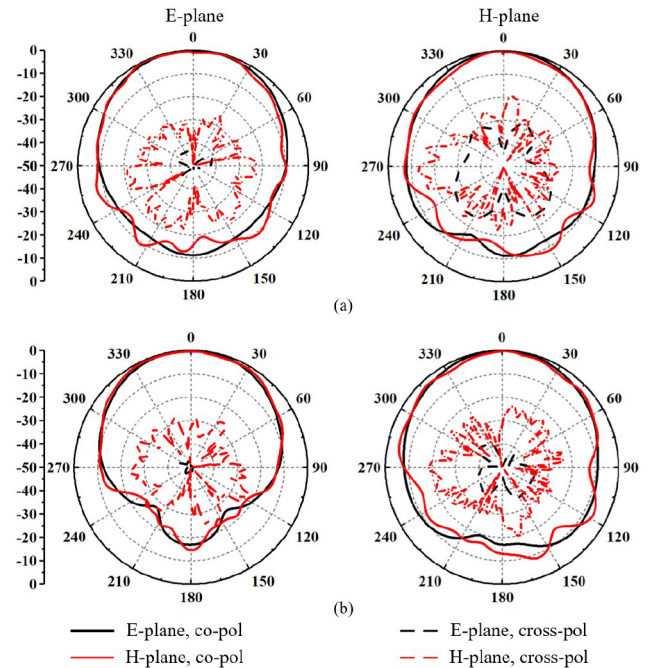

FIGURE 7. Simulated and measured radiation patterns of the proposed LP DRA. (a) 9.3 GHz. (b) 10.4 GHz.

simulation. Here, all the other parameters are fixed as the final values. It can be observed that as ε_{r2} increases, the frequency of TE_{131} mode decreases rapidly while that of TE_{111} mode only slightly moves downward. The spacing between the two modes, therefore, becomes small, making them easy for combination. It can also be from Fig. 4(a) that the influence from dielectric changing on TE_{111} mode becomes gradually weak with the increase of g. This is because that the increase of g makes the dielectric strip more concentrated in margin area of Region B, where the E-field intensity of TE_{111} mode is much weaker. Fig. 4(b) further plots the frequency ratio change of the two target modes, where we can find that the slope of curve $g = 0$ is changing from positive to negative with the increasing of ε_{r2}, and the slope of curve $g = 0.4$ mm is relatively small, while only the curves of $g = 0.8$ mm and $g = 1.2$ mm have large and steady slopes. This indicates that for the cases of $g = 0.8$ mm and $g = 1.2$ mm, the TE_{131} mode can be shifted down rapidly and smoothly to approach the TE_{111} mode when ε_{r2} is increased. With the above analysis, ε_{r2} and g can be selected. The permittivity of the dielectric strips ε_{r2} is suggested to be larger than 57 to keep the two resonances close to each other. We chose $\varepsilon_{r2} = 69$ in this design according to the material list of our processor. The air gap is finally set as $g = 0.8$ mm considering both factors of that TE_{111} mode should be less affected while TE_{131} mode should be significantly and linearly affected.

Fig. 5(a) shows the simulated frequencies of TE_{111} mode and TE_{131} mode at different dielectric strip height h_4. Here, all the other parameters are fixed as the final values. It is observed that as h_4 increases, the frequency of TE_{131} mode shifts down, while the frequency of TE_{111} mode remains relatively stable. It is reasonable since increasing the volume of DR is a similar means as increasing its permittivity to bring down the resonant frequencies. Fig. 5(b) clearly depicts the merging process of the two modes from the perspective of reflection coefficient.

It can be concluded that by properly modifying the dielectric characteristics of Region B, that is tuning parameters of ε_{r2}, g, and h_4, the frequency of TE_{131} mode can be significantly affected and shifted down to merge with that of TE_{111} mode which is less affected. As a result, extended operating bandwidth can be obtained without enlarging the DR planar size.

D. SIMULATED AND MEASURED RESULTS

To verify the design concept of the proposed antenna, an LP DRA prototype was fabricated and measured. Fig. 6(a) exhibits the photograph of the antenna prototype, while Fig. 6(b) shows the measured and simulated $|S_{11}|$ and gain results. As can be learned, the measured impedance bandwidth for $|S_{11}| < -10$ dB is 17.3% (9.12 $\sim$ 10.84 GHz). The measured gain of the antenna is stable, which is more than 6.2 dBi across the bandwidth with a peak gain of 7.1 dBi identified at $\sim$10.4 GHz. The measured and simulated radiation patterns in E-plane and H-plane at 9.3 GHz and 10.4 GHz are presented in Fig. 7. The measured cross-polarization levels within the 3-dB beam widths are lower than -18 dB at 9.3 GHz, and -22 dB at 10.4 GHz, respectively. Generally, reasonable agreement has been achieved between the simulated and measured results.

To achieve high gain and beam-scanning capability, a linear 1×5 antenna array is designed with the proposed LP DRA element. Fig. 8. shows the configuration of the antenna
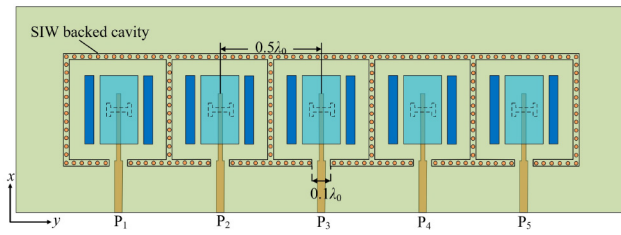
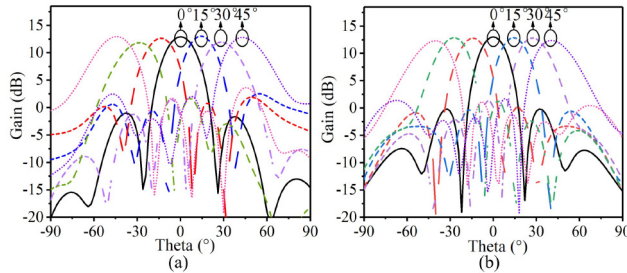**FIGURE 8.** The geometric configuration of the 1 × 5 LP DRA array.

FIGURE 9. The simulated beam scanning performance of LP DRA array at different frequency. (a) 9.5 GHz. (b) 10.5 GHz.
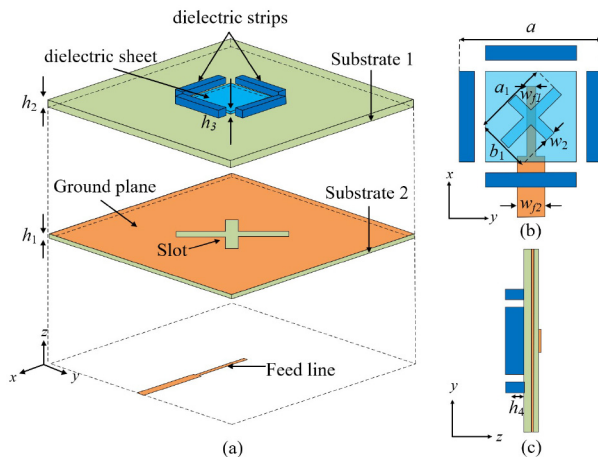

FIGURE 10. Configuration of the proposed CP DRA. (a) 3-D view. (b) Top view. (c) Side view. (Design parameters: $h_1 = 0.508$, $h_2 = 0.813$, $h_3 = 0.45$, $h_4 = 2$, $a = 10$, $a_1 = 8$, $b_1 = 5.6$, $w_{f1} = 0.55$, $w_{f2} = 1.2$, $w_2 = 0.32$. Units: mm.)
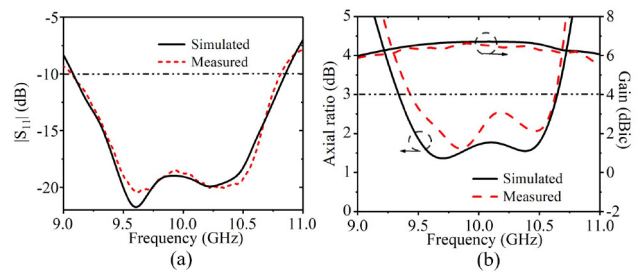

FIGURE 11. Simulated and measured results of the CP DRA. (a) |S$_{11}$|. (b) AR and gains.
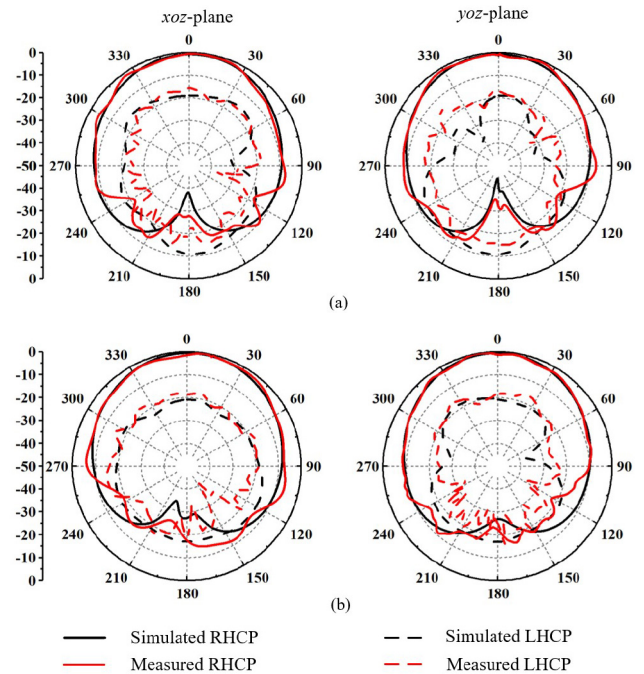
FIGURE 12. Simulated and measured radiation patterns of the CP DRA. (a) 9.5 GHz. (b) 10.5 GHz.

array. The spacing between each two elements is set to be 14.8 mm, which corresponds to 0.5 λ_0 at 10.5 GHz. To reduce the mutual coupling, substrate integrated waveguide (SIW) backed cavities are introduced to surround the DRA elements. Beam-scanning capability can be obtained by phasing the array with progressive phase shifts between the elements. Fig. 9(a) and (b) show the simulated 2-D radiation patterns of the array at 9.5 GHz and 10.5 GHz, respectively. It is learned that the maximum realized gains in broadside direction is 12.9 dBi and 13 dBi at 9.5GHz and 10.5GHz, respectively. In the horizontal plane, the beam can be steered ±45° at the two frequencies before the criteria of a 3-dB scan loss or −10-dB sidelobe level is met. As the scan angle exceeds ±45°, decreased gain drops of more than 3dB or increased sidelobe levels of higher than −10 dB appear in numerical simulation.

III. CIRCULARLY POLARIZED ANTENNA DESIGN

The proposed technique can be further extended for a CP antenna design. Fig. 10 shows the configuration of the CP antenna. The basic structure of the CP design is kept almost the same as that of the LP antenna. Some adjustments have been made for achieving CP radiation, which are described as follows:

1) Two dielectric strips located on two sides have been changed into two pairs of dielectric strips distributed over all of the sides. This is because that, for the case of CP radiation, the effect from the modification of dielectric material should be imposed simultaneously on the degenerated modes along orthogonal directions (x-axis and y-axis).

2) The feeding slot has been changed to a cross-slot with unequal arms for excitation of degenerate modes with equal amplitudes and 90° phase differences.

A CP DRA prototype was fabricated and measured. Fig. 11 shows the measured and simulated |S$_{11}$|, ARs and gains of the CP antenna. The −10 dB impedance bandwidth
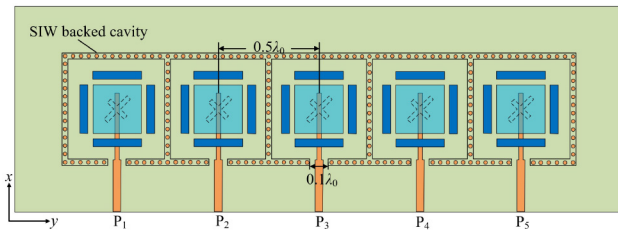
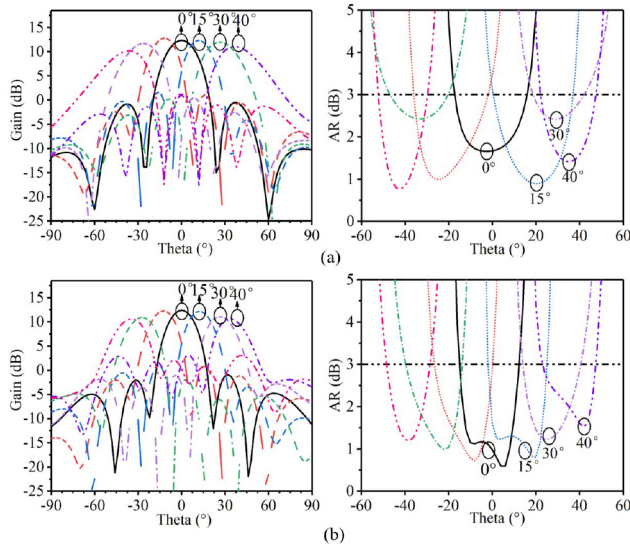**FIGURE 13.** The geometric configuration of the 1 × 5 CP DRA array.

FIGURE 14. Simulated beam scanning performance and ARs of the CP DRA array in the *yoz* plane at (a) 9.5 GHz and (b) 10.5 GHz.

is 17.5% (9.07 ∼ 10.81 GHz), and the AR bandwidth is 12% (9.4 ∼ 10.6 GHz), which is fully within the impedance bandwidth. A peak gain of 6.6 dBic is achieved at 9.9 GHz. Fig. 12 depicts the radiation patterns in *xoz* and *yoz* planes at 9.5 GHz and 10.5 GHz, respectively. The cross-polarization levels are lower than −14 dB at 9.5 GHz, and −15 dB at 10.5 GHz within the 3-dB beam widths.

As shown in Fig. 13, a 1 × 5 antenna array is also designed with the proposed CP antenna element. Fig. 14(a) and (b) show the simulated 2-D radiation patterns and ARs of the array at 9.5GHz and 10.5GHz, respectively. It is learned that the maximum realized gains in broadside direction is 12.3 dBi and 12.4 dBi at 9.5 GHz and 10.5 GHz, respectively. In the *yoz* plane, the beam can be steered ±40° at the two frequencies before the criteria of a 3-dB scan loss or −10-dB sidelobe level is met. As scanning angle increases from 0° to 15° at 9.5 GHz, the 3-dB AR beamwidth increases from 32° to 38°. It then decreases to 24° with the scanning angle increased to 40°. Different from the results at 9.5 GHz, the 3-dB AR beam beamwidth of the antenna array at 10.5 GHz is relatively steady, varying from 21°∼28°.

IV. CONCLUSION

In this paper, a kind of compact and low-profile DRA with extended bandwidth is proposed. This kind of antenna is

designed with its TE_{111} and TE_{131} modes. It has been shown that by properly tuning the dielectric parameters of the designated region, the high-order TE_{131} mode, which is originally far away from the dominant mode, can be pulled down to combine with the TE_{111} mode, yielding an extended bandwidth. The operating mechanism is presented to illustrate the antenna concept. Based on the basic antenna, a CP design is further proposed. To verify the idea, antenna prototypes have been constructed and measured and shown to match well with the simulated results. The proposed DRA is designed for potential beam-scanning and low profile applications. With this application background, the antenna shows an enhanced operating bandwidth comparing to its competitors. Besides, the proposed technique can be applied in both LP and CP design, showing a good versatility.

REFERENCES

[1] S. Yoshida *et al.*, "A 60-GHz band planar dipole array antenna using 3-D SiP structure in small wireless terminals for beamforming applications," *IEEE Trans. Antennas Propag.*, vol. 61, no. 7, pp. 3502–3510, Jul. 2013.

[2] S. C. Swales, M. A. Beach, D. J. Edwards, and J. P. McGeehan, "The performance enhancement of multibeam adaptive base-station antennas for cellular land mobile radio systems," *IEEE Trans. Veh. Technol.*, vol. 39, no. 1, pp. 56–67, Feb. 1990.

[3] J. G. Andrews *et al.*, "What will 5G be?" *IEEE J. Sel. Areas Commun.*, vol. 32, no. 6, pp. 1065–1082, Jun. 2014.

[4] B. Yang, Z. Yu, Y. Dong, J. Zhou, and W. Hong, "Compact tapered slot antenna array for 5G millimeter-wave massive MIMO systems," *IEEE Trans Antennas Propag.*, vol. 65, no. 12, pp. 6721–6727, Dec. 2017.

[5] F. Abushakra, A. Al-Zoubi, I. Al-Hmoud, T. Walpita, and N. Jeong, "Wideband and high efficiency 64-element RDRA array for radar applications," *IEEE Open J. Antennas Propag.*, vol. 2, pp. 932–936, 2021.

[6] N. K. Darimireddy, R. R. Reddy, and A. M. Prasad, "Wideband circularly polarized cylindrical dielectric resonator antennas with rectangular curved slots [antenna applications corner]," *IEEE Antennas Propag. Mag.*, vol. 62, no. 6, pp. 65–73, Dec. 2020.

[7] S. A. Long, M. W. McAllister, and L. C. Shen, "The resonant cylindrical dielectric cavity antenna," *IEEE Trans. Antennas Propag.*, vol. 31, no. 3, pp. 406–412, May 1983.

[8] A. Petosa, *Dielectric Resonator Antenna Handbook.* Boston, MA, USA: Artech, 2007.

[9] M. Rad, N. Nikkhah, B. Zakeri, and M. Yazdi, "Wideband dielectric resonator antenna with dual circular polarization," *IEEE Trans. Antennas Propag.*, vol. 70, no. 1, pp. 714–719, Jan. 2022.

[10] Z. Chen, Q. Liu, B. Sanz-Izquierdo, H. Liu, J. Yu, and X. Chen, "A wideband circular-polarized beam steering dielectric resonator antenna using gravitational ball lens," *IEEE Trans. Antennas Propag.*, vol. 69, no. 5, pp. 2963–2968, May 2021.

[11] H. I. Kremer, K. W. Leung, and M. W. K. Lee, "Design of substrate-integrated dielectric resonator antenna with dielectric vias," *IEEE Trans. Antennas Propag.*, vol. 69, no. 9, pp. 5205–5214, Sep. 2021.

[12] S. Gupta, A. Sharma, G. Das, R. K. Gangwar, and M. Khalily, "Wideband circularly polarized dielectric resonator antenna array with polarization diversity," *IEEE Access*, vol. 7, pp. 49069–49076, 2019.

[13] U. Illahi *et al.*, "Design of new circularly polarized wearable dielectric resonator antenna for off-body communication in WBAN applications," *IEEE Access*, vol. 7, pp. 150573–150582, 2019.

[14] S. Liu, D. Yang, Y. Chen, S. Huang, and Y. Xiang, "Broadband dual circularly polarized dielectric resonator antenna for ambient electromagnetic energy harvesting," *IEEE Trans. Antennas Propag.*, vol. 68, no. 6, pp. 4961–4966, Jun. 2020.

[15] J. Kowalewski, J. Eisenbeis, A. Jauch, J. Mayer, M. Kretschmann, and T. Zwick, "A mmW broadband dual-polarized dielectric resonator antenna based on hybrid modes," *IEEE Antennas Wireless Propag. Lett.*, vol. 19, pp. 1068–1072, 2020.

[16] Y. Al-Alem and A. A. Kishk, "Wideband millimeter-wave dielectric resonator antenna with gain enhancement," *IEEE Antennas Wireless Propag. Lett.*, vol. 18, pp. 2711–2715, 2019.

[17] X. S. Fang, K. P. Shi, and Y. X. Sun, "Design of the single-/dual-port wideband differential dielectric resonator antenna using higher order mode," *IEEE Antennas Wireless Propag. Lett.*, vol. 19, pp. 1605–1609, 2020.

[18] M. Wang and Q.-X. Chu, "A wideband polarization-reconfigurable water dielectric resonator antenna," *IEEE Antennas Wireless Propag. Lett.*, vol. 18, pp. 402–406, 2019.

[19] H. W. Lai, K.-M. Luk, and K. W. Leung, "Dense dielectric patch antenna—A new kind of low-profile antenna element for wireless communications," *IEEE Trans. Antennas Propag.*, vol. 61, no. 8, pp. 4239–4245, Aug. 2013.

[20] A. Rashidian, L. Shafai, M. Sobocinski, J. Peräntie, J. Juuti, and H. Jantunen, "Printable planar dielectric antennas," *IEEE Trans. Antennas Propag.*, vol. 64, no. 2, pp. 403–413, Feb. 2016.

[21] M. Asaadi and A. Sebak, "Gain and bandwidth enhancement of 2×2 square dense dielectric patch antenna array using a holey superstrate," *IEEE Antennas Wireless Propag. Lett.*, vol. 16, pp. 1808–1811, 2017.

[22] N. Yan, K. Ma, and H. Fu, "A high-permittivity dielectric material-filled SISL antenna with cavity backing," *IEEE Trans. Wireless Antennas Propag. Lett.*, vol. 20, pp. 1033–1037, 2021.

[23] Y. M. Pan and S. Y. Zheng, "A low-profile stacked dielectric resonator antenna with high-gain and wide bandwidth," *IEEE Antennas Wireless Propag. Lett.*, vol. 15, pp. 68–71, 2015.

[24] X.-Y. Wang, S.-C. Tang, L.-L. Yang, and J.-X. Chen, "Differential-fed dual-polarized dielectric patch antenna with gain enhancement based on higher order modes," *IEEE Trans. Antennas Propag.*, vol. 19, no. 3, pp. 502–506, Mar. 2020.

[25] Y. Liu, H. Liu, M. Wei, and S. Gong, "A low-profile and high-permittivity dielectric resonator antenna with enhanced bandwidth," *IEEE Antennas Wireless Propag. Lett.*, vol. 14, pp. 791–794, 2014.

[26] L. Guo and K. W. Leung, "Compact linearly and circularly polarized unidirectional dielectric resonator antennas," *IEEE Antennas Wireless Propag. Lett.*, vol. 64, pp. 2067–2074, 2016.

[27] Z. Chen *et al.*, "Millimeter-wave rectangular dielectric resonator antenna array with enlarged DRA dimensions, wideband capability, and high-gain performance," *IEEE Antennas Wireless Propag. Lett.*, vol. 68, pp. 3271–3276, 2020.

[28] W.-J. Sun, W.-W. Yang, P. Chu, and J.-X. Chen, "Design of a wideband circularly polarized stacked dielectric resonator antenna," *IEEE Trans. Antennas Propag.*, vol. 67, no. 1, pp. 591–595, Jan. 2019.

[29] K. Xu and J. Shi, "High-efficiency circular dense dielectric patch antenna with frequency selectivity," *Electron. Lett.*, vol. 54, no. 14, pp. 861–862, 2018.

[30] W. M. Abdel-Wahab, M. Abdallah, J. Anderson, Y. Wang, H. Al-Saedi, and S. Safavi-Naeini, "SIW-Integrated parasitic DRA array: Analysis, design, and measurement," *IEEE Antennas Wireless Propag. Lett.*, vol. 18, pp. 69–73, 2019.

[31] S.-J. Guo, L.-S. Wu, K. W. Leung, and J.-F. Mao, "Microstrip-fed differential dielectric resonator antenna and array," *IEEE Antennas Wireless Propag. Lett.*, vol. 17, pp. 1736–1739, 2018.

[32] N. K. Darimireddy and C.-W. Park, "Electromagnetic coupled circularly polarized hybrid antenna for LTE applications," in *Proc. IEEE Int. Symp. Antennas Propag. North Amer. Radio Sci. Meeting*, 2020, pp. 401–402.

[33] M. Haneishi and H. Takazawa, "Broadband circularly polarised planar array composed of a pair of dielectric resonator antennas," *Electron. Lett.*, vol. 21, no. 10, pp. 437–438, May 1985.

[34] N. K. Sahu, G. Das, R. K. Gangwar, and R. Karumudi, "An arrangement for four-element MIMO DRA with complementary CP diversity," *IEEE Antennas Wireless Propag. Lett.*, vol. 20, pp. 1616–1620, 2021.

[35] R. Chowdhury and R. K. Chaudhary, "An approach to generate circular polarization in a modified cylindrical-shaped dielectric resonator antenna using PMC boundary approximation," *IEEE Antennas Wireless Propag. Lett.*, vol. 17, pp. 1727–1731, 2018.

[36] M. Elahi, A. Altaf, Y. Yang, K.-Y. Lee, and K. C. Hwang, "Circularly polarized dielectric resonator antenna with two annular vias," *IEEE Access*, vol. 9, pp. 41123–41128, 2021.

[37] J.-X. Chen, X.-Y. Wang, Y.-X. Huang, L.-L. Yang, and S.-C. Tang, "A low-profile circularly polarized dielectric patch antenna with bandwidth expansion," *Int. J. RF Microw. Comput.-Aided Eng.*, vol. 31, no. 3, Dec. 2021, Art. no. e22526.

JIE-ER ZHANG was born in Nantong, Jiangsu, China, in 1999. He received the B.S. degree in electronic science and technology from Nantong University Xinglin College, Nantong, in 2021. He is currently pursuing the M.S. degree with the School of Materials Science and Engineering, Yancheng Institute of Technology. His current research interest is microwave antenna.

QINFANG ZHANG was born in Danyang, Jiangsu, China, in 1980. He received the B.S. degree from Xuzhou Normal University, Xuzhou, Jiangsu, China, in 2000, and the M.S. and Ph.D. degrees from Nanjing University, Nanjing, China, in 2005. Since 2012, he has been with the Yancheng Institute of Technology, Yancheng, Jiangsu, China, where he is currently a Professor. He has authored or coauthored more than 100 internationally referred journal and conference papers. He holds 19 Chinese patents and 1 U.S. patent. His research interests include development and application of cluster beam deposition technology and materials informatics.

WEIBIN KONG received the B.S. degree in mathmatics from Qufu Normal University, China, in 2007, and the M.S. degree in mathmatics and the Ph.D. degree in radio engineering from Southeast University, Nanjing, China, in 2010 and 2015, respectively.

Since 2016, he has been with the School of the College of Information Engineering, Yancheng Institute of Technology, Yancheng, China, where he is currently an Associate Professor. His research interests include the IE-based domain decomposition method, the FFT-based fast algorithm, the hybrid algorithm for multiscale EM problems, and deep learning.

WEN-WEN YANG (Member, IEEE) received the B.Eng. degree in information engineering and the M.Eng. and the Ph.D. degrees in electrical engineering from Southeast University, Nanjing, China, in 2007, 2010 and 2015, respectively.

Since 2015, he has been with the School of Electronics and Information, Nantong University, Nantong, China, where he is currently an Associate Professor. From August 2018 to August 2019, he was a Visiting Researcher with Polytechnique Montréal, Montreal, Canada. He has authored or coauthored more than 50 internationally referred journal and conference papers. His research interests include RF, microwave and millimeter-wave passive devices, active antenna array, and antennas for wireless communication. He serves as a reviewer for several IEEE and IET journals.

JIAN-XIN CHEN (Senior Member, IEEE) was born in Nantong, Jiangsu, China, in 1979. He received the B.S. degree from Huaiyin Teachers College, Huaiyin, Jiangsu, China, in 2001, the M.S. degree from the University of Electronic Science and Technology of China, Chengdu, China, in 2004, and the Ph.D. degree from the City University of Hong Kong, Hong Kong, in 2008.

Since 2009, he has been with Nantong University, Nantong, where he is currently a Professor. He has authored or coauthored more than 100 internationally referred journal and conference papers. He holds 25 Chinese patents and 3 U.S. patents. His research interests include microwave active/passive circuits and antennas, LTCC-based microwave and millimeter-wave filters and devices, and dielectric resonator filters and antennas. He was a recipient of the New Century Excellent Talents in University of the Ministry of Education for China in 2011. He was the supervisor of several conference best paper award winners.